Gyre-scale circulation cells in the Red Sea

Detlef QUADFASEL [a] and Horst BAUDNER [b]

[a] Institut für Meereskunde der Universität Hamburg, Troplowitzstr. 7, 2000 Hamburg 54, Germany.

[b] Deutscher Wetterdienst, Seewetteramt Hamburg, Bernhard-Nocht Straße 76, 2000 Hamburg 36, Germany.

ABSTRACT

High resolution synoptic hydrographic surveys carried out during 1982 to 1987 are used to delineate the two-dimensional baroclinic flow pattern of the Red Sea. It is shown that the circulation can be characterized through a succession of four gyres, some 200 km in diameter, the locations of which are linked to the major topographic basins of the Red Sea. The gyres have a transport almost an order of magnitude larger than the large-scale thermohaline driven flow. They appear to be forced by the strongly rotational wind field over the Red Sea.

Oceanologica Acta, 1993. **16**, 3, 221-229.

RÉSUMÉ

Cellules de circulation à l'échelle de bassins en Mer Rouge

A partir de campagnes de mesures hydrologiques synoptiques de haute résolution réalisées entre 1982 et 1987, il a été possible de restituer un schéma bidimensionnel de la circulation barocline en Mer Rouge. Cette circulation se caractérise par un ensemble de quatre «gyres» de 200 km de diamètre dont l'emplacement est déterminé par le relief bathymétrique des principeaux bassins de la Mer Rouge. Les transports associés aux différents «gyres» sont d'un ordre de grandeur supérieurs au transport associé à la circulation thermohaline de grande échelle. Il semble que l'existence de ces «gyres» doive être attribuée au fort rotationnel de vent caractérisant cette région.

Oceanologica Acta, 1993. **16**, 3, 221-229.

INTRODUCTION

The large-scale circulation within the Red Sea is governed by strong thermohaline and wind forces, each of which is extreme with respect to normal oceanic scales. An excess of evaporation over precipitation of more than 2 m/a (Privett, 1959) leads to near-surface salinities higher than 41 in the north and, together with winter cooling, drives a thermohaline flow in the upper and deep layers (Phillips, 1966; Manins, 1973; Maillard, 1971; Wyrtki, 1972). The atmospheric forcing is, at least in the southern part, dominated by bi-annually reversing monsoon winds that give

rise to seasonally changing patterns of the upper layer circulation (Siedler, 1969; Patzert, 1974).

The relative importance of these mechanisms has been much debated after the observational data from the International Indian Ocean Expedition became available. Siedler (1969) compared direct transport measurements in the Strait of Bab El Mandeb with estimates of the exchange with the Indian Ocean from mass and salt budget calculations of the entire Red Sea. Within measurement uncertainties both values were comparable, suggesting a dominant thermohaline driven exchange with the Gulf of Aden. On the other hand, Patzert (1974) found a close correlation of
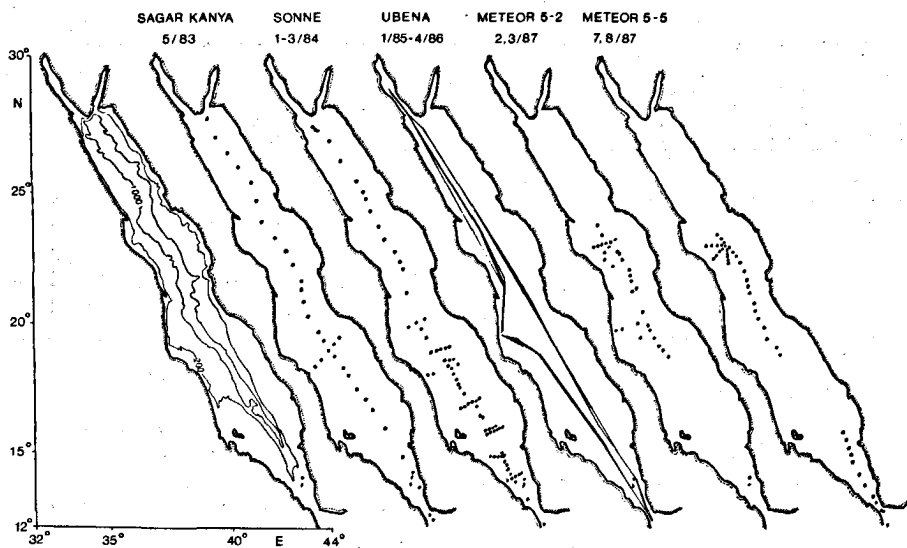
the flow field with the monsoonal wind forcing, causing a two layer structure to develop during winter and a three-layer structure with intermediate depth inflow during summer. This pattern was confirmed with direct current measurements by Maillard and Soliman (1986). Thus it appears that the vertical structure of the flow is strongly influenced by the wind forcing while the overall exchange of Red Sea Water is controlled by the evaporative loss of fresh water.

These climatological characteristics of the Red Sea, both atmospheric and oceanic, have been described in a number of articles from a two-dimensional viewpoint (Siedler, 1969; Morcos, 1970; Patzert, 1974; Maillard and Soliman, 1986). The channel approach is understandable as the Red Sea basin is about 2000 km long but on average only 220 km wide. Also, most oceanographic measurements were taken only along its central axis, restricting the analysis to along-basin variations.

However, the lateral variability cannot be neglected when discussing the circulation within the Red Sea. Maillard (1971) and earlier Neumann and McGill (1962) documented the existence of three-dimensional structures of the hydrographic and flow fields that indicated either a meandering of the mean flow or even a succession of closed circulation cells. Surface current speeds in these features measured by the geomagnetic electro-kinetograph (GEK) were up to 0.5 m/s (Maillard, 1971), by far exceeding the climatogical mean along-axis flow of only about 0.1 m/s (Patzert, 1974). Additional evidence for the existence of these structures comes from a three-dimensional baroclinic circulation model (König, 1982: General circulation model of the Red Sea, Technical Report RS 1, Institut für Meereskunde, Universität Hamburg, 56 pp.,unpublished

manuscript) that shows a succession of cyclonic and anti-cyclonic gyres with diameters corresponding to the width of the Red Sea.

To study the structure and dynamics of the circulation in detail, a series of hydrographic surveys was carried out by the Institut für Meereskunde, Hamburg, between 1983 and 1987. The aim of this investigation was to determine
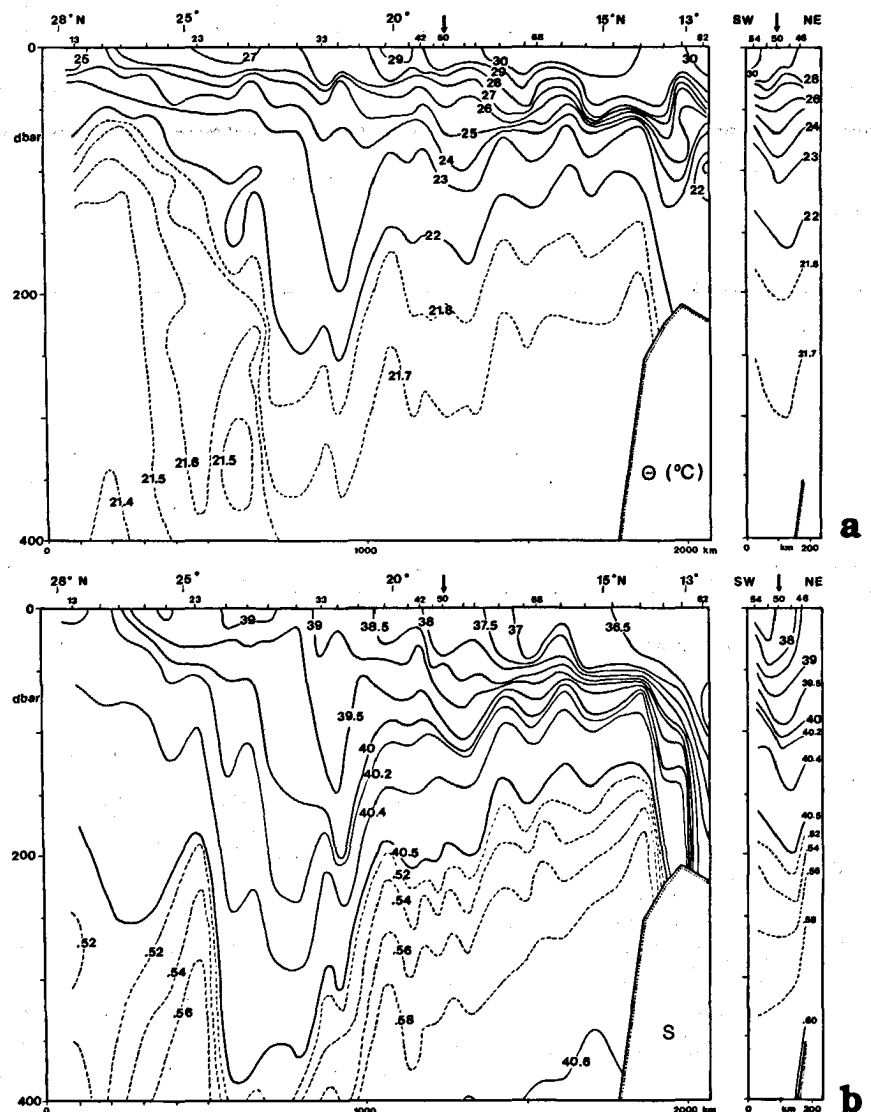
whether the eddies or gyres are transient features or if they form an integral part of the large-scale circulation of the Red Sea. A second question concerns their forcing mechanism: are they some kind of instability of the mean flow; are they directly wind forced; or are they controlled by the local topography, as suggested by Wyrtki (1972)?

DATA

The hydrographic data used are temperature and salinity profiles measured with a ME-Multisonde conductivity-temperature-depth sonde (CTD) and temperature profiles from expendable bathythermographs (XBTs). The CTD profiles were calibrated with salinity probes obtained from a rosette sampler and with reversing thermometer readings. Accuracies are better than 0.01 K for temperature and 0.01 for salinity. The XBT profiles were checked against surface readings from bucket samples and against the temperature of the Red Sea Deep Water (21.6 ± 0.1 °C). Resulting accuracies are better than 0.2 K.

The data were collected during four research cruises and during an XBT-ship of opportunity programme:

● R.V. *Sagar Kanya* cruise 1 (May 1983): one CTD/XBT section along the central axis of the Red Sea, one cross-section at 18° N. The CTD data are compiled *in* Baudner, Jancke and Quadfasel, 1984 (CTD-data obtained in the Red Sea during 21-30 May 1983, R.V. Sagar Kanya. Technical Report 1-84, Institut für Meereskunde der Universität Hamburg, 63 pp., unpublished manuscript).

● R.V. *Sonne* cruise 29 (January-March 1984): one along-axis CTD/XBT section, nine cross-sections south of 21° N. A detailed, repeated survey was conducted near 19° N. Due to malfunctioning of the conductivity cell only the temperature profiles from the CTD casts can be used.

● MCS *Ubena* (January 1985-April 1986): fourteen XBT sections along the axis of the trench at approximately one month intervals. During some of the transects the track departed from the axis between 18° N and 22° N due to port calls in Port Sudan (Quadfasel and Verch, 1987: Seasonal variability of temperature in the Red Sea: XBT-sections from MCS *Ubena* in 1985 and 1986. Technical Report 1-87, Institut für Meereskunde, Universität Hamburg, 25 pp., unpublished manuscript).

● R.V. *Meteor* cruise 5/2 (February-March 1987): one partial along axis CTD section (18°-24° N), two cross-sections
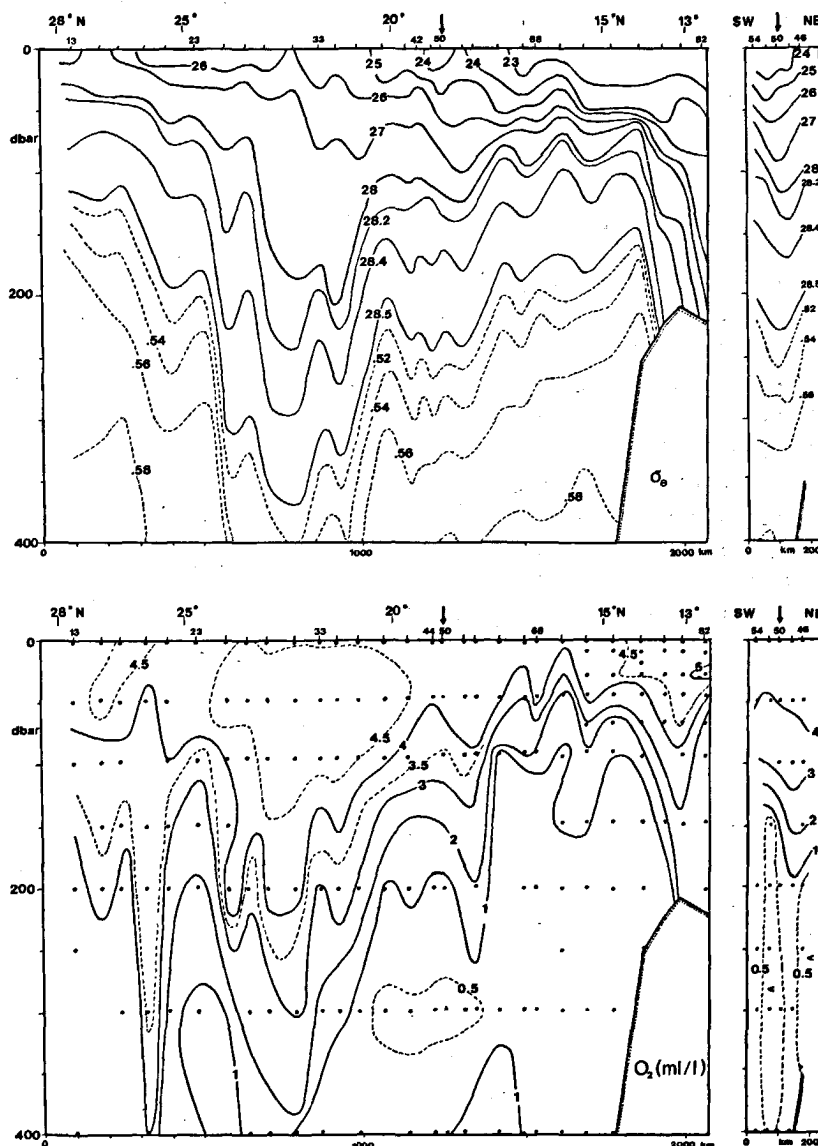

Figure 2

Vertical distribution of potential temperature (°C), salinity, potential density (10^{-3} kg/m³) and dissolved oxygen content (ml/l) in the upper 400 m of the water column during May 1983. Left: section along the main axis of the Red Sea. Right: cross-section near 18° N.

near 23° N (Verch *et al.*, 1989: Mindik 1987-R.V. *Meteor* cruise 5: CTD observation in the Red Sea and the Gulf of Aden. Technical Report 1-89, Institut für Meereskunde, Universität Hamburg, 151 pp., unpublished manuscript).

• R.V. *Meteor* cruise 5/5 (July-August 1987): one partial along axis CTD section (12°-16° N, 18°-24° N), three cross-sections near 23° N (Verch *et al.*, 1989).

The location of the CTD and XBT sections are shown in Figure 1 together with the bathymetry of the Red Sea.

In addition we will use CTD data obtained in 1982 from R.V. *Marion Dufresne* (Maillard and Soliman, 1986) and historical XBT/BT data, available from NODC Washington.

HYDROGRAPHIC CONDITIONS DURING MAY 1983

To map the spatial distribution of mesoscale features in the upper layer of the Red Sea an along-axis hydrographic section between the Gulf of Suez and the Strait of Bab El Mandeb and a cross-section near 18° N with closer station spacing (20-40 km) were occupied in May 1983 by R.V. *Sagar Kanya*. Figure 2 shows the vertical distribution of potential temperature, salinity, potential density and dissolved oxygen content along these sections.

The large scale pattern resembles well the climatological picture given by Patzert (1974), the stratification is typical for the transition from the NE to the SW-monsoon. Surface temperatures are highest just north of Bab El Mandeb (30°C) decreasing to 25°C in the north. Surface salinities increase from 36.5 in the south to more than 40 in the north, manifesting the evaporative freshwater loss of the inflowing water from the Indian Ocean.

The flow regime at Bab El Mandeb is still that of the NE monsoon, with a two-layer structure. No intrusion of cold water can be seen at intermediate depths. Oxygen values show a pronounced minimum around 300 m depth in the southern part of the Red Sea, a result of the balance between upwelling of Red Sea Deep Water and downward diffusion of surface water (Wyrtki, 1972).

The most striking features with respect to scales less than the basin length are, however, the strong depressions of the thermo- and haloclines near 22° and 18° N. The 22°C isotherm and the 40.25 isohaline drop to depths of more than 250 m near 22° N compared to a level of 100-150 m in the south. The oxygen values here are also far higher than in the neighbouring areas. The strongest depression of the isopycnals is found slightly further north, near 23° N. The pycnocline depression at 18° N is also associated with high temperatures, low salinities and a higher oxygen content, but appears to be confined to the upper 200 to 150 m of the water column.

These two features are indicative of anticyclonic eddies or gyres in the circulation. At least for the southern eddy this is supported by the distribution of hydrographic parameters along the cross-section (Fig. 2) that likewise shows a thermo- and halocline depression in its centre. Figure 3 shows the horizontal distribution of the geopotential anomaly of the surface relative to 400 dbar, the deepest common pressure level in the area of the southern gyre, and the depth of the 24°C isotherm. The error in the geopotential anomaly due to internal waves or other high frequency variability is less than 0.8 dyn cm, as estimated from a 21-hour station, during which 10 CTD profiles were taken at the same location. For the 24°C isotherm map also XBT profiles, collected in between CTD stations, were used. Both maps show closed isolines, indicative of a closed circulation pattern. The gyre has a horizontal scale of 150-200 km, similar to the one near 23° N which corresponds closely to the width of the Red Sea. This scale of the circulation cells is much larger than the baroclinic deformation radius, which here is of order 30 km, and compares favourably with the wave length of the cellular structures found previously (Maillard, 1971).

Horizontal transports within these gyres were calculated from geostrophic estimates of the velocity profiles, taking 400 dbar as reference level. In all cases the strongest vertical shear was found in the pycnocline between 50 and 150 m depth, below 200 m the shear was negligible. In the surface mixed layer the shear is in the same direction in opposing parts of the sections, presumably due to non-geostrophic frictional effects. During the survey the mean wind was towards the north with a speed of 6 m/s, resulting in an Ekman transport τ/f of 0.20 x 10^6 m³/s per 100 km, corresponding to a mean speed of 0.04 m/s over 50 m depth. Here τ is the surface wind stress and f the Coriolis parameter.
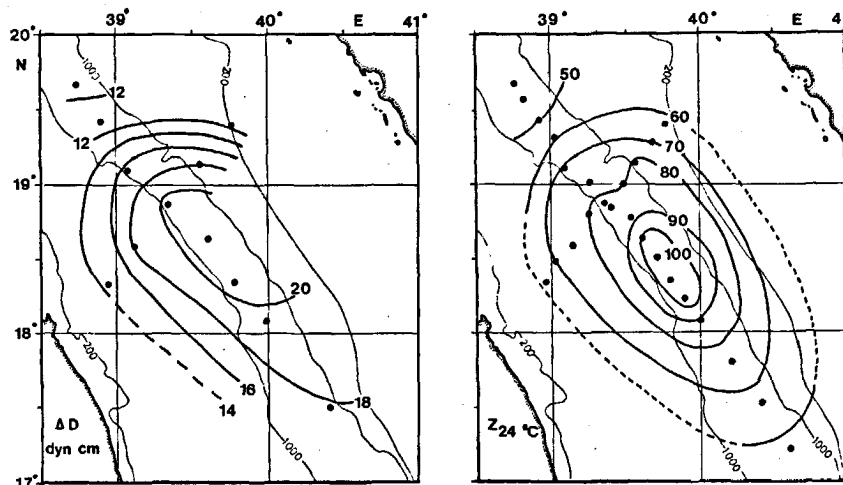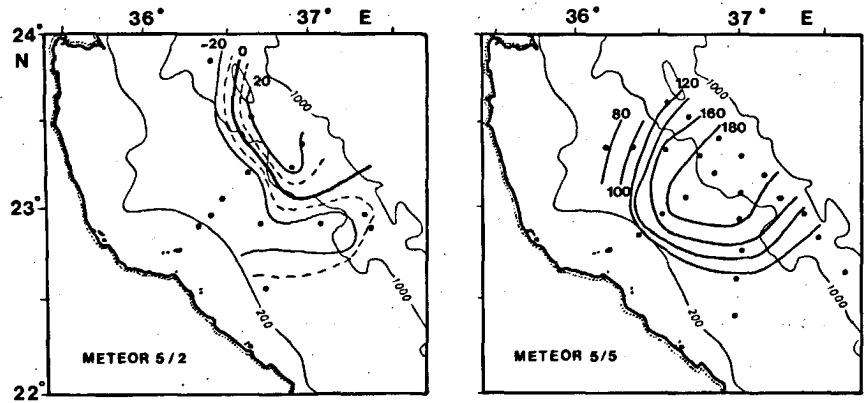
Figure 3

Geopotential anomaly of the sea surface relative to 400 dbar (in dyn cm) and depth of the 24 °C isotherm (in meters) in the southern (18° N) gyre during May 1983. Data is hand-contoured.

Figure 4

Geopotential anomaly (in dyn mm) of the sea surface relative to 400 dbar in the 23° N gyre during February and August 1987. Data is hand-contoured.

The Ekman current agrees with the shear values seen in the geostrophic velocity profiles in the upper mixed layer.

The mean circular transport in the upper 100 m of the southern gyre (18° N) averaged over the four radial sections is $1.4 \pm 0.1 \times 10^6$ m³/s. The northern gyre (23° N) has an average transport of $2.6 \pm 0.3 \times 10^6$ m³/s. These values are significantly larger than the mean transports along the main axis of the Red Sea and exchanges with the Gulf of Aden which have been estimated to range from 0.21 and 0.33×10^6 m³/s (Siedler, 1969; Patzert, 1974; Maillard and Soliman, 1986).

GYRE SURVEYS NEAR 23° N

During R.V. *Meteor* cruise 5 two detailed hydrographic surveys of the northern 23° N gyre were carried out in February and July 1987. No working permissions were granted for the eastern half of the basin, so the survey had to be restricted to Sudanese territorial waters, covering only the western part of the gyre. The distribution of the geopotential anomaly of the sea surface relative to 400 dbar is given in Figure 4.
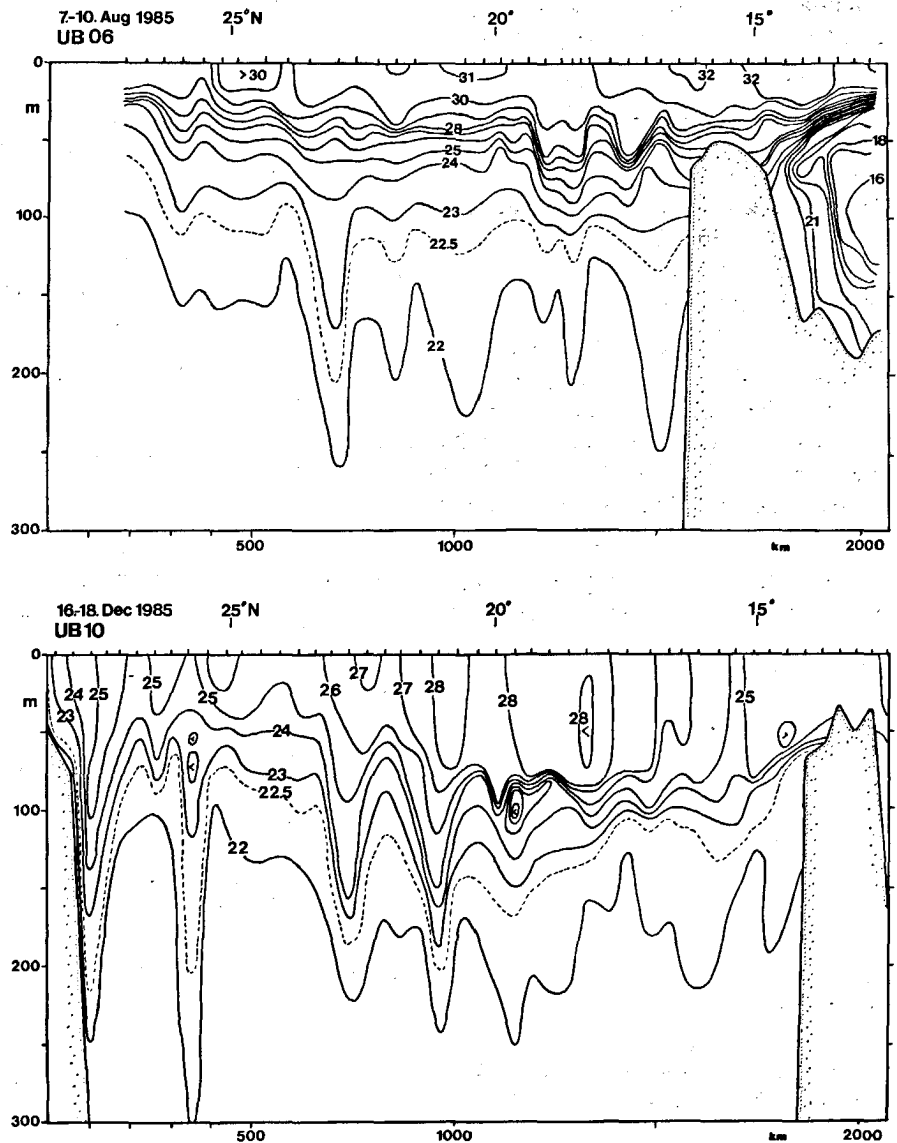

Figure 5

XBT temperature sections along the main axis of the Red Sea collected during the height of the monsoon seasons in August and December 1985.

During July the anticyclonic gyre is well resolved by the station distribution, its centre is located near 23° 15' N, 37° 00' E. Geostrophic surface currents calculated relative to 400 dbar exceed values of 0.6 m/s and the transport across the five radial section in the upper 100 m is $1.4 \pm 0.2 \times 10^6$ m³/s. During February the centre of the gyre has shifted somewhat more to the north-east and is resolved only by eight hydrographic stations. Surface currents are less than 0.3 m/s and also the upper layer transports are only about half of those of the summer survey ($0.6 \pm 0.1 \times 10^6$ m³/s). However, these low transport values may only reflect that the gyre was not properly resolved.

SEASONAL VARIABILITY DURING 1985-1986

The strong signature of the gyres in the temperature field makes it possible to detect them from temperature data alone. To obtain some statistics about the existence, scale and location of the gyres over the course of a seasonal cycle, an XBT ship of opportunity programme was run from January 1985 to April 1986, covering the central axis of the Red Sea (Quadfasel and Verch, 1987, unpublished, *op. cit.*). Sippican Deep Blue expendable bathythermographs were launched from MCS *Ubena* at nominally 90 minute-intervals while the vessel was on transit from the Gulf of Suez to Bab El Mandeb. This corresponds to a horizontal separation of the profiles between 30 and 40 km. The probes were deployed from the wing of the navigation bridge (24 m height) on the leeward side of the vessel, using a standard hand-launcher system. The data were digitally logged on a micro computer equipped with an XBT interface (Emery *et al.*, 1986). During twelve of the fourteen transects the vessel called in Port Sudan (19° 40' N), causing a westward deviation of the trackline from the central axis of the Red Sea. Thus, data from the region between 19° and 21° N may not be representative of Red Sea open water conditions.

Temperature sections from the height of the two monsoon seasons are shown as examples in Figure 5. In August 1985 strong thermocline depressions were found near 23° and 18° N where gyres were observed during the *Sagar Kanya* hydrographic survey. In December a deepening of the isotherms was also found at 26° and 21° N, in addition to the one at 23° N. South of 20° N the picture is obscured by the intrusion of cold water from the Indian Ocean that spreads into the Red Sea at intermediate depths (70-100 m) in the three-layer current system at Bab El Mandeb (Patzert, 1974).

The distribution of the isotherm depressions and their seasonal variability are more clearly seen in Figure 6, where the depth of the 22 °C isotherm has been plotted in a time-latitude diagram. A persistent depression exists at 23°-24° N with depths of more than 200 m throughout the 16 months of the measurements. A second deep band, although not quite as pronounced, stretches at around 20°-21° N and a third one at 17°-18° N.

The persistence of these depressions, in particular near 23° N, shows that the gyres are not intermittent, short-lived features but seem to form an integral part of the circulation of the Red

Sea. The noisier structure in the southern part of the Red Sea may have two reasons. In the first place, the gyres here have a smaller vertical extent and often do not reach into the deeper part of the thermocline. On the other hand, the intrusion of cold intermediate water from the Indian Ocean that reaches as far north as 18° N during the SW monsoon in summer may distort the picture. The low salinity of this water more strongly influences the density, and the shape of the pycnocline cannot be inferred from temperature data alone.

INVENTORY OF THE GYRES

To obtain more comprehensive statistics of the gyres, all available data from the Red Sea have been scanned for synoptic hydrographic sections that have a resolution good enough to detect gyres. Apart from the data described above, complete hydrographic data (T and S) are available only from the *Marion Dufresne* cruise in 1982 (Maillard and Soliman, 1986). In addition, 8 XBT/BT temperature sections were found in the NODC files up to 1979.

These sections were then scanned for thermocline depressions or upliftings with an horizontal scale between 150 and 300 km, indicative of anticyclonic or cyclonic eddies. Altogether 49 anticyclonic and 4 cyclonic eddies were identified in the 28 synoptic hydrographic sections. Their location and horizontal extent is shown in Figure 7 in a time-latitude diagram.

Two main points emerge:
- 50 of the 53 gyres are concentrated in four latitude bands: 17°-19° N, 19°-21.5° N, 21.5°-24° N and 24°-27° N. Only three gyres were centred on the boundaries of the above latitude bands.

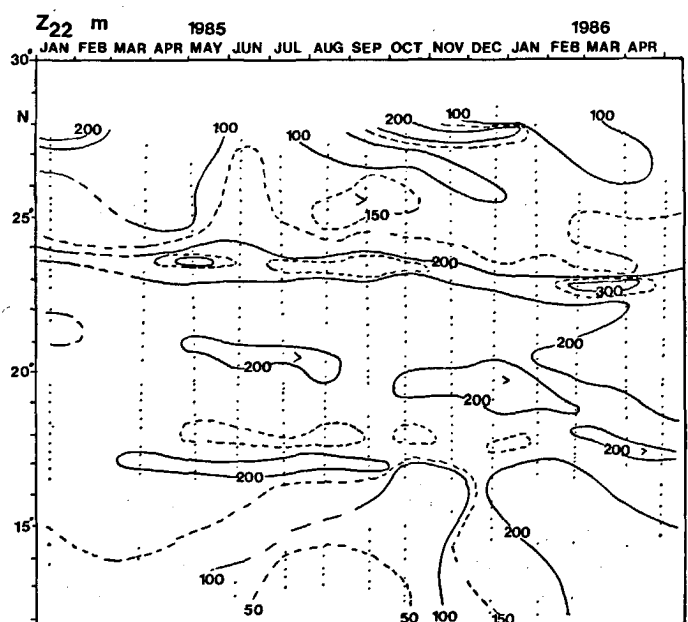Figure 6

Time-latitude diagram of the depth of the 22 °C isotherm during January 1985 to April 1986, based on 14 XBT sections.
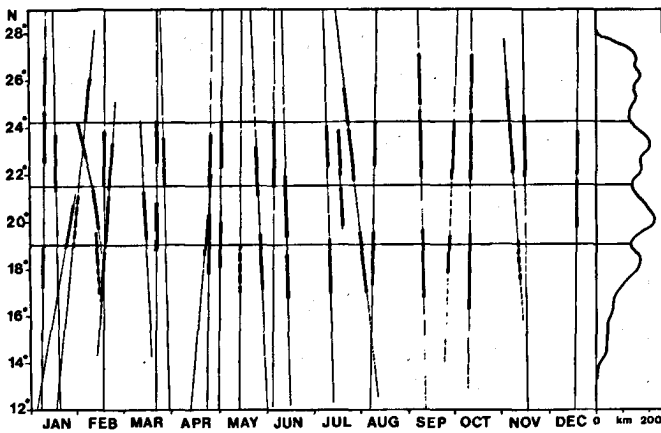
Figure 7

Time-latitude diagram of the distribution (location and extent) of gyres detected in synoptic hydrographic and XBT sections. Solid lines indicate anticyclonic, broken lines cyclonic features. The graph on the right indicates the lateral width of the Red Sea, taken as the distance between the 200 m isobaths.

- Cyclonic eddies were only found south of 21° N and only during the winter months at the time of the NE monsoon.

On the right hand side of Figure 7 we plotted the lateral width of the Red Sea, taken as the distance between the 200 m isobaths. It shows that the Red Sea consists of four wider basins, their separating narrows coincide with the boundaries between the latitude bands where most of the gyres are observed. Thus, it appears that the gyres are somewhat linked to these basins, *i. e.* they are topographically trapped.

Baroclinic geostrophic transports can be calculated only when both temperature and salinity data are available. The close coupling of the pycnocline topography to the thermocline topography, however, makes it possible to estimate gyre transports also in those cases, when only temperature data are available. For the 21.5°-24° N latitude band where sufficient hydrographic data are available, we have correlated the geostrophic gyre transports (0-100 m) relative to 400 dbar with the differences between the 22 °C isotherm depths in the centre and the rim of the gyres (Fig. 8).

Using this regression, transports were estimated for the 17 "temperature gyres". Together with the geostrophic estimates given above, a mean transport of $2.1 \pm 0.9 \times 10^6$ m^3/s results. A seasonal cycle of transports which may be expected due to the monsoonal variability of the forcing field cannot be detected in the data due to the large variability within the individual months.

GENERATION OF THE GYRES

Thermohaline and wind forces drive the large-scale (two-dimensional) circulation of the Red Sea (Patzert, 1974; Phillips, 1966; Siedler, 1969). The observed gyres are three-dimensional and are associated with transports in the upper layer that are significantly larger than that of the mean along axis flow. They preferably exist in the wide basins of the Red Sea and thus appear to be topographically trapped. So the question arises as to what mechanism is responsible for the generation of these gyres.

Instabilities of the mean flow can be ruled out as the observed scale is by far too large. The thermohaline forcing is basinwide and not active on the 200 km scale. Thus, wind forcing and interaction with the local topography remain as a possibility.

The dominant component of the surface wind field is in the along-axis direction (Patzert, 1974), guided by the high mountains and plateaus on either side of the basin. Figure 9 shows the along-axis component of the surface wind stress in a time-latitude diagram, based on wind data from ship observations compiled in 1° x 1° latitude-longitude squares by Cadet (unpublished). In the southern part
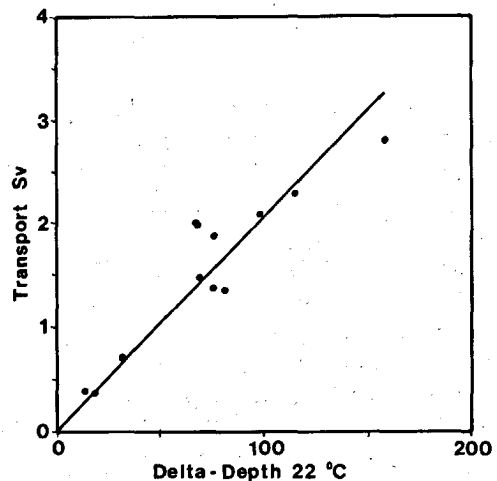

Figure 8

Relation between the geostrophic gyre transports in the upper 100 m (relative to 400 dbar) and the depth difference of the 22 °C isotherm at the centre and the rim of the 23° N gyres.
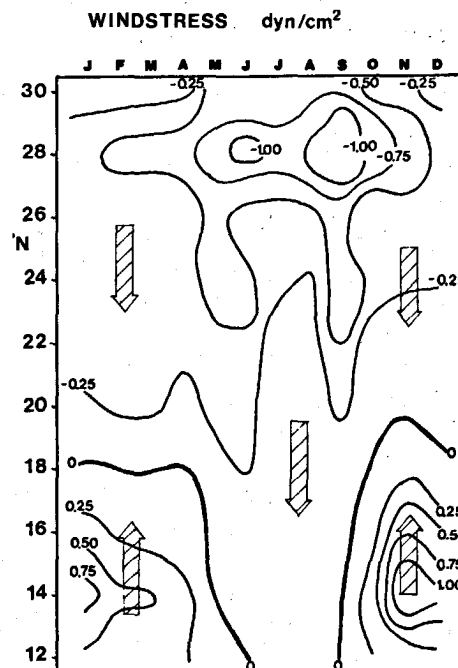

Figure 9

Seasonal development of the along-axis component of the surface wind stress (Cadet, unpublished). The data is based on a thirteen-year time series of monthly mean surface wind observations from ships, averaged over 1° x 1° latitude-longitude squares.

the wind field reverses twice per year. During the SW monsoon from June to September the winds blow SSE while during the NE monsoon and the transition times between the monsoon periods (October to May) the air-
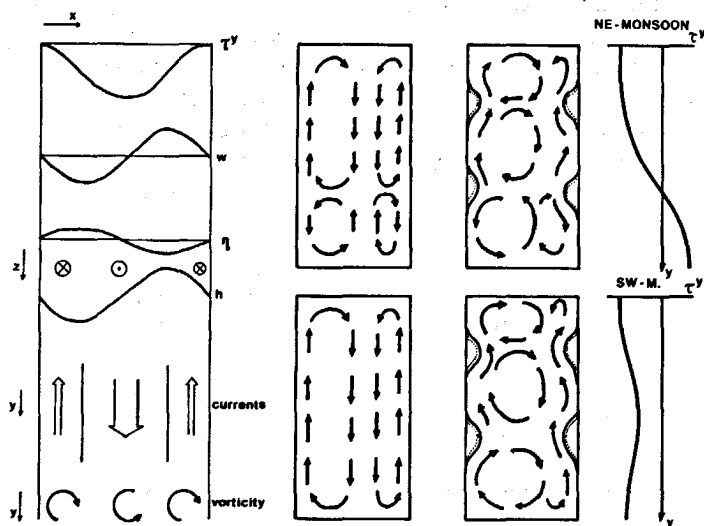

Figure 10

Schematic representation of the dynamics for the northerly wind case and resulting circulation during the two monsoon seasons for a rectangular basin and a basin with topographic narrows. Left panel: lateral distribution of meridional windstress τʸ; resulting Ekman pumping velocity w; height of sea surface and depth of thermocline h; surface currents; and vorticity generation due to variation of Coriolis parameter. Centre panel: surface circulation during the SW monsoon in a rectangular basin and one with topographic narrows included. Right panel: same for NE monsoon. The meridional variation of the windstress τʸ during the two seasons is given on the far right.
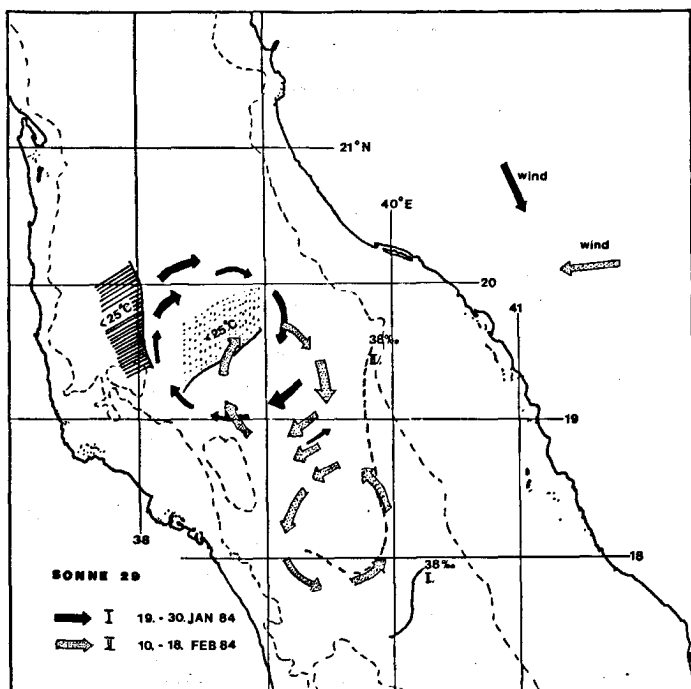

Figure 11

Schematic representation of the circulation near 19° N as inferred from the thermocline topography during January and February 1984. Areas with sea surface temperature below 25°C and location of the 38 isohaline at the surface during the two periods are indicated.

flow is directed NNW. North of about 20° N the wind is blowing SSE throughout the year, being strongest during summer and weakest during winter.

Laterally the mean wind stress decreases strongly from the central axis towards the boundaries on either side, due to lateral friction effects, although the detailed shape of the profile can not be determined from the coarse grid of the monthly averages.

Assuming the profile to have a sinusoidal shape as given in Figure 10, the resulting wind-driven circulation can be inferred. The rotation of the wind field causes upwelling in the eastern and downwelling in the western part of the basin. Ekman pumping velocities are largest at about one-quarter of the channel width away from the coastal boundaries and the associated slope of the sea surface will, in the case of northerly winds, drive two northward coastal currents and a broader southward current in the centre (Fig. 10). Due to the variation of the Coriolis parameter with latitude, the northward branches acquire anticyclonic vorticity and the southward branch cyclonic vorticity. This leads to an eastward shift of the boundaries between the current regimes. The western northward flow broadens and the width of the eastern northward flow is reduced. For the case of southerly winds (NE monsoon, south of 20° N) the same arguments apply, with the currents being reversed but still be shifted to the east.

The resulting pattern of the near-surface circulation during the two monsoon periods is shown schematically in the centre panel of Figure 10. In each of the wind domains two elongated circulation cells exist, with the western one being somewhat broader. In the realistic case for the Red Sea with topographic narrows (Fig. 10, right panel) the boundary flows will be forced into a meridional direction and it does not seem to be unreasonable to suggest that part of the flow recirculates directly, giving rise to closed circulation cells or gyres.

Although the model described is rather simple, not taking into account the complicated bottom topopography of the Red Sea (Fig. 1), the resulting circulation resembles the observed distribution of gyres rather well. Cyclonic features have only been observed south of 21° N in January, February, May and November, *i. e.* during the NE monsoon in the region of cyclonic wind forcing (Fig. 7, 9). North of the wind convergence and during the SW monsoon only anticyclonic gyres have been observed, in agreement with the model prediction.

The effectiveness of the local wind forcing in setting up a gyre-scale circulation was observed during the winter 1984 campaign of R.V. *Sonne*. The near surface circulation as inferred from the thermocline topography is shown schematically in Figure 11. In January the wind convergence was located near 18° N with northerly winds (8 m/s) north of that latitude. Centred at 19.5° N was an anticyclonic eddy, the northern extension of which was not fully covered during this survey. During mid-February the wind convergence zone had shifted northward and weak (< 5 m/s) easterly winds prevailed in the area. The anticy-

clonic eddy had weakened and shrunk in size, but near 18° N a cyclonic feature had developed. The uplifting of the thermocline in its centre was somewhere between 15 and 25 m depth, depending on which outer boundary it was referred to. The cyclonic curl associated with the wind field was 4×10^{-8} dynes/cm^3. Assuming this curl to have acted over the period of fourteen days between the two hydrographic surveys implies an uplifting due to Ekman pumping of

$$\Delta h = \int w \, dt = 1/\rho f \int curl \, \tau \, dt = 15 \text{ m}.$$

Here w is the Ekman pumping velocity, ρ the density and f the Coriolis parameter. Thus, the local rotation of the wind field appears to be able to generate the gyre-scale circulation cells that are observed in the various basins of the Red Sea.

REFERENCES

Emery W.J., W. Lee, W. Zenk and J. Meincke (1986). A low-cost digital XBT system and its application to the real-time computation of dynamic height. *J. atmos. ocean. Technol.*, **3**, 75-83.

Maillard C. (1971). Étude hydrologique et dynamique de la Mer Rouge en hiver. *Annls Inst. océanogr., Paris*, **498**, 2, 113-140.

Maillard C. and G. Soliman (1986). Hydrography of the Red Sea and exchanges with the Indian Ocean in summer. *Oceanologica Acta*, **9**, 3, 249-269.

Manins P.C. (1973). A filling box model of the deep circulation of the Red Sea. *Mém. Soc. r. Sci. Liège*, **6**, 6, 153-166.

Morcos S.A. (1970). Physical and chemical oceanography of the Red Sea. *Oceanogr. mar. Biol. a. Rev.*, **8**, 223-235.

Neuman A.C. and D.A. McGill (1962). Circulation of the Red Sea in summer. *Deep-Sea Res.*, **8**, 223-235.

Patzert W.C. (1974). Wind induced reversal in the Red Sea circulation. *Deep-Sea Res.*, **21**, 109-121.

Phillips O.M. (1966.) On turbulent convection currents and the circulation of the Red Sea. *Deep-Sea Res.*, **13**, 1149-1160.

Privett D.W. (1959). Monthly charts of evaporation from the North Indian Ocean, including the Red Sea and Persian Gulf. *Q. Jl R. met. Soc.*, **85**, 424-428.

Siedler G. (1969). General circulation of water masses in the Red Sea. in: *Hot brines and recent heavy metal deposits in the Red Sea*, E.T. Degens and D.A. Ross, editors. Springer N.Y., 131-137.

Wyrtki K. (1972). On the deep circulation of the Red Sea. *Colloque international du CNRS*, **215**, 91-106.